

PHYSICS OPPORTUNITIES IN THE FAR-FORWARD REGION AT THE FUTURE ELECTRON-ION COLLIDER*

ALEXANDER JENTSCH

Department of Physics, Brookhaven National Laboratory
Upton, New York 11973, USA
ajentsch@bnl.gov

*Received 3 April 2023, accepted 5 April 2023,
published online 6 September 2023*

The Electron-Ion Collider provides the opportunity to drastically advance our understanding of QCD and the multidimensional structure of both protons and nuclei. An essential component of the EIC physics program is the identification and characterization of exclusive, diffractive, and tagged events using detectors integrated with the outgoing hadron beam-line, the so-called “far-forward” detectors. The ePIC experiment includes a suite of far-forward detectors designed to deliver the necessary geometric coverage and resolution required to achieve the exclusive physics program envisioned at the EIC. In addition to the multidimensional imaging program at the EIC, topics such as spectator tagging in $e + d$ and $e + {}^3\text{He}$ reactions to access structure functions and searches for gluon saturation in $e + A$ collisions are also enabled by this experimental apparatus. In these proceedings, the ePIC far-forward detectors will be briefly introduced, and a few selected physics topics focused on tagged deep-inelastic scattering will be discussed.

DOI:10.5506/APhysPolBSupp.16.7-A13

1. Introduction

The future Electron-Ion Collider (EIC) is slated to begin construction in the summer of 2025 in the United States at Brookhaven National Laboratory in Upton, New York. This new machine will yield unprecedented access to studies of nuclear physics via deep-inelastic scattering (DIS) reactions of electrons with protons and light and heavy ions — all while providing for the capability for high luminosity ($\sim 10^{34} \text{ cm}^{-2}\text{s}^{-1}$) and polarization ($\sim 75\%$) of both the electron and proton (light-ion) beams. Of particular interest is the access to exclusive and diffractive reactions afforded by a comprehensive

* Presented at the 29th Cracow Epiphany Conference on *Physics at the Electron-Ion Collider and Future Facilities*, Cracow, Poland, 16–19 January, 2023.

set of state-of-the-art detectors which instrument the hadron-going beam-line and provide for an entire physics program centered around partonic imaging, nuclear structure, and other related topics. These detectors — the so-called “far-forward” detectors — enable the reconstruction of both charged and neutral final-state particles in four subsystems leveraging silicon tracking technology and electromagnetic/hadronic calorimetry. A description of the physics program and the detector and accelerator design considerations can be found in the EIC Yellow Report [1] and EIC Conceptual Design Report [2]. In July of 2022, the ePIC Collaboration was formed with the goal of providing the structure and scientific support needed to realize the first EIC detector. The ePIC Collaboration has rapidly built up a management structure to help ensure on-time delivery of a Technical Design Report, required for construction on the EIC to begin.

In these proceedings, I will give an overview of the detector systems and technologies, and provide a few examples of relevant physics topics and studies, especially those which go beyond the originally proposed program in the EIC White Paper [3].

2. Far-forward detectors

The EIC far-forward detectors are comprised of four independent subsystems, as shown in Fig. 1. The various subsystems are integrated directly into the outgoing hadron beam-line, which poses distinct experimental

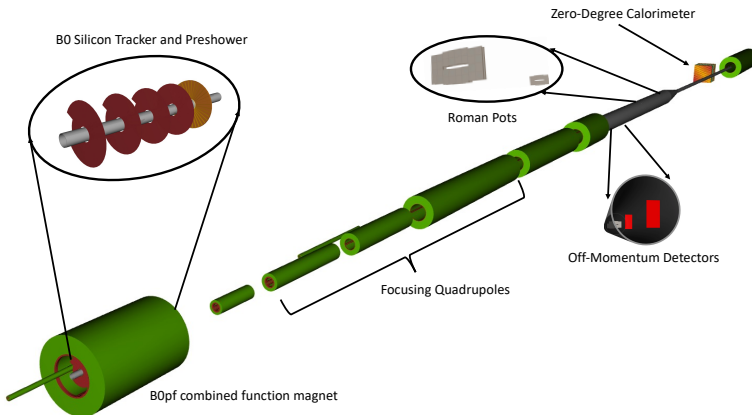


Fig. 1. The layout of the EIC far-forward area showing the four detector subsystems. A few of the relevant beam-line magnets are also labeled for reference. The magnets are combinations of bending dipoles and focusing quadrupoles. A schematic beam pipe is included in the drawing. The interaction point (IP) is at the bottom left, and the hadron beam direction is from left to right in the figure. Layout generated using the ePIC DD4hep simulation framework [4].

challenges for both the detectors and operations of the EIC machine. Table 1 summarizes the geometric acceptance for far-forward protons and neutrons achieved with the present design [1]. Note that x_L here refers to the longitudinal momentum fraction of the protons with respect to the settings for the accelerator dipole magnets. Lower x_L generally references particles which come from knockout reactions in nuclei.

Table 1. Summary of the geometric acceptance for far-forward protons and neutrons in polar angle θ and longitudinal momentum fraction x_L , provided by the baseline EIC far-forward detector design [1].

Detector	Used for	θ accep. [mrad]	x_L accep.
B0 tracker	p	6.0–20.0	N/A
Off-Momentum	p	0.0–5.0	0.45–0.65
Roman Pots	p	0.0–5.0	0.6–0.95*
Zero-Degree Calorim.	n	0.0–4.5	N/A

*The Roman Pots acceptance at high values of x_L depends on the optics choice for the machine.

In the following, I summarize the main features of the subsystems as relevant to the present studies, in the order in which they appear when moving away from the interaction point, as seen in Fig. 1. Additional details can be found in Refs. [1, 2, 5, 6].

2.1. B0 spectrometer and calorimeter

The B0 detector is a multi-functional subsystem comprised of a cutting-edge silicon tracking detector and a high-resolution PbWO4 electromagnetic calorimeter (EMCAL), see Fig. 2. The tracking system will consist of three layers of MAPS silicon with $\sim 10 \mu\text{m}$ spatial resolution based on the ALICE ITS3 upgrade. Additionally, one layer of AC-coupled low-gain avalanche diodes (AC-LGADs), which provide the required timing resolution (~ 35 ps) needed to disentangle background events and the impact of the EIC crab crossing, will be included in the tracking subsystem. The whole system is embedded in the first dipole magnet after the interaction point for the ePIC Detector (B0pf magnet), creating a fully-functional tracking spectrometer out of an EIC accelerator magnet. This subsystem is optimized for reconstructing charged particles with polar scattering angles of $6.0 < \theta < 20.0$ mrad, such as large-angle protons from nuclear breakup. The B0 tracking detector provides p_T -resolution of 2–5% for protons with $p \sim 100$ GeV/c, with the majority of smearing coming from beam effects, such as angular divergence.

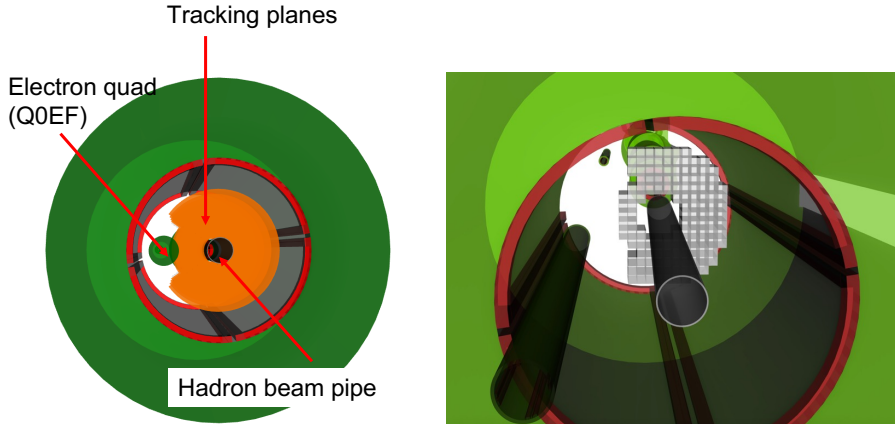


Fig. 2. Detector geometry for the B0 spectrometer (left) and EMCAL (right) produced using ePIC DD4hep simulations [4]. Engineering support structure is not currently included in the simulations in DD4hep, but will require re-running of physics simulations for impact assessment in the very near future.

The EMCAL is composed of 7 cm long PbWO₄ crystals, which are 2.5 cm \times 2.5 cm in the transverse size. This subsystem provides percent-level energy resolution for the reconstruction of photons from $\pi^0 \rightarrow \gamma\gamma$ decays, and for tagging photons from $e + A$ collisions to veto incoherent reactions.

2.2. Roman Pots

The Roman Pots are designed to reconstruct protons from exclusive reactions where the longitudinal momentum fraction, x_L , of the protons with respect to the beam is $> 60\text{--}65\%$. An ePIC DD4hep rendering of one of the Roman Pots stations is shown in Fig. 3. The EIC Roman Pots are implemented in a way that is different from previous experiments in that they are proposed not to use the “pot” vessel which normally protects these detectors, but serves as an impediment to full detector acceptance at low- p_T . The lack of the vacuum pot vessel means care must be taken to protect the detector from stray RF power, and also to protect the EIC accelerator from impedance effects from the presence of the detectors in the beam-line vacuum. In light of this, work is underway to engineer a shielding system which solves both of these problems, while still allowing for the necessary acceptance and basic performance of the subsystem. The subsystem is arranged in two stations, separated by two meters, each with two planes of detectors for redundancy and background rejection.

The Roman Pots subsystem also makes use of the AC-LGAD technology used in the B0 tracking system to provide both the necessary timing (~ 35 ps) and spatial resolution (~ 140 μm) required by the physics pro-

gram. Reconstruction of particles using the Roman Pots is carried out using a transfer matrix which describes charged particle trajectories through the accelerator magnets.

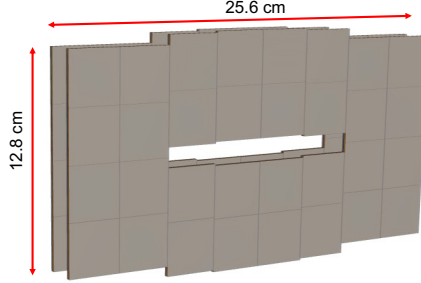


Fig. 3. Detector geometry for the Roman Pots detector package using ePIC DD4hep simulations [4].

2.3. Off-Momentum Detectors

The Off-Momentum Detectors (OMD) follow the same essential design principles as the Roman Pots, but are located in a prime location for reconstruction of protons from nuclear breakup reactions (*e.g.* spectators from $e + d$ deep-inelastic scattering). The OMD subsystem is shown in Fig. 4.

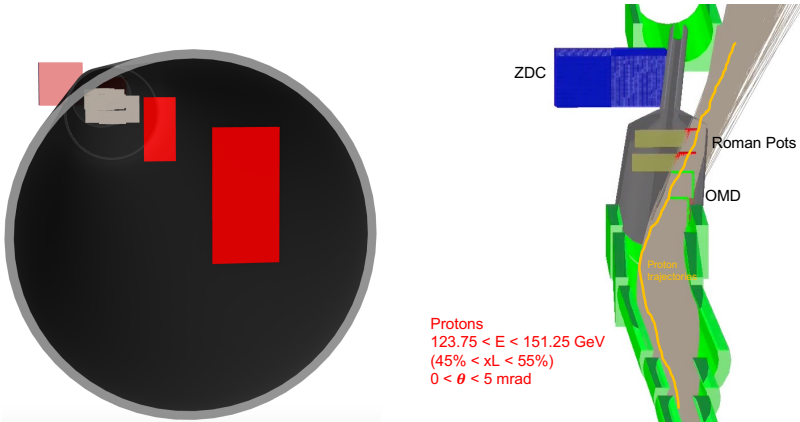


Fig. 4. Detector geometry for off-momentum detector package using ePIC DD4hep simulations (left) and EICRoot simulation (right) [8]. The right panel shows a group of protons whose momentum is on average 50% of the beam momentum (*e.g.* $x_L \sim 0.5$). These protons are bent more severely by the accelerator dipole magnets and often miss the Roman Pots entirely, necessitating another subsystem in the Off-Momentum Detectors.

Additionally, the OMDs are required to allow for additional vetoing power for $e + A$ reactions, where separation of coherent events from incoherent background requires vetoing efficiencies above 95% [7].

2.4. Zero-Degree Calorimeter

The Zero-Degree Calorimeter (ZDC) consists of both electromagnetic and hadronic calorimetry, and is based on the ALICE FoCAL detector concept [9]. The present design for the EIC application is shown in Fig. 5. The EIC ZDC uses both Pb + silicon and Pb + scintillator sampling calorimeters for hadrons, and has a hadronic energy resolution of at least $\frac{50\%}{\sqrt{E}} \oplus 5\%$, and a position resolution of ~ 1.3 mm.

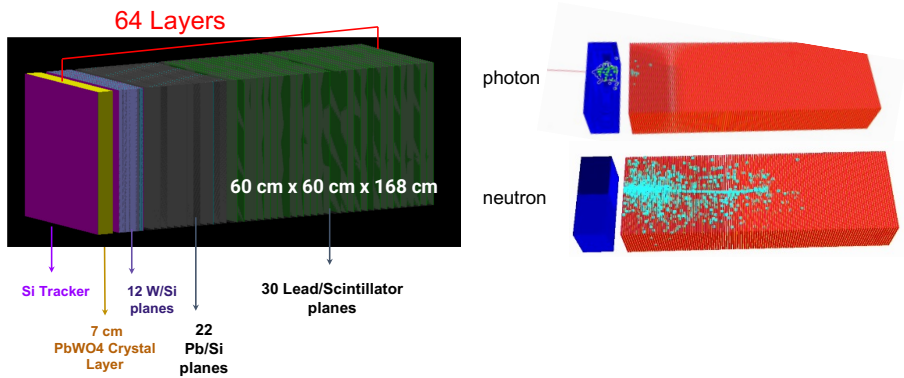


Fig. 5. Detector geometry for the Zero-Degree Calorimeter using ePIC DD4hep simulations [4] (left), and examples of photon and neutron showers in EMCAL + HCAL layers from a standalone Geant4 simulation (right). The right plot is to illustrate the difference in the shower formation for hadrons and depict the challenge in designing a high-resolution detector.

Studies are ongoing to further improve the energy resolution for hadronic reconstruction, especially with respect to transverse shower leakage present for hadrons with $\theta > 2$ mrad. Photon reconstruction is carried out using both a PbWO4 crystal calorimeter and a W + silicon imaging system.

Furthermore, studies are underway to optimize the use of shower imaging in the ZDC to accurately reconstruct transverse hadron momenta, and also to make use of advanced machine learning methods to account for shower leakage and apply corrections to the energy deposits in the detector used to reconstruct the particle energy.

3. Selected physics topics

3.1. BeAGLE Monte-Carlo Generator

In all of the studies concerning the deuteron and presented in these proceedings, the BeAGLE Monte-Carlo Generator [10] has been used to generate the Monte-Carlo samples which are then passed through the full detector simulations to create a full analysis. For the deuteron case, BeAGLE uses PYTHIA 6 [11] to simulate the primary scattering process (*e.g.* deep-inelastic scattering, J/ψ production), while the spectator kinematics are parameterized using a particular description of the deuteron spectral function [12]. The final events are then passed through two different detector simulation frameworks, EICRoot [8] or the ePIC framework [4], to apply both the detector and beam effects to the simulated events.

3.2. Short-range correlations

Short-range two-nucleon correlations (SRCs) are an important topic of study in nuclear physics and are one of the possible explanations for the origin of the EMC effect (see Section 3.4). In establishing prospects for the potential reach of the EIC for an SRC physics program, a comprehensive study of exclusive J/ψ production was carried out, with a focus on the experimental capabilities for both spectator and active nucleon reconstruction [13].

Figure 6 shows both generator-level and reconstructed longitudinal and transverse momenta for the spectator neutron (leading proton). This reconstruction is done with the ZDC, with the smearing being dominated by a combination of both the ZDC energy resolution and beam effects (angular divergence).

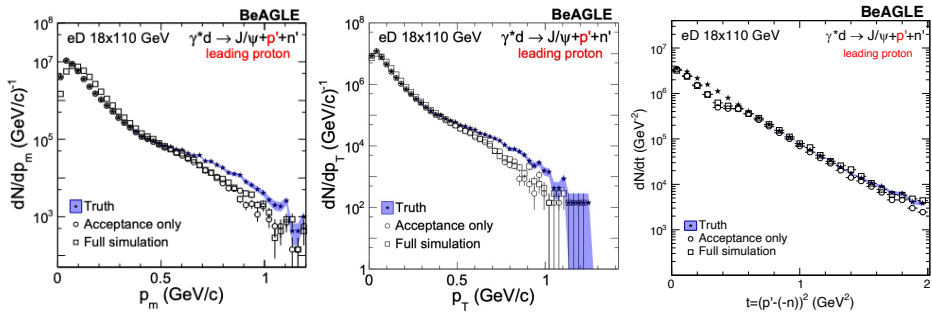


Fig. 6. Kinematic distributions for spectator neutron reconstruction in exclusive J/ψ production, *cf.* [13]. The left and middle plots show the reconstruction longitudinal and transverse momentum of the spectator neutrons, respectively. The right plot shows the momentum transfer, t -distribution using reconstructed momentum for both the spectator neutron and active proton.

Another promising aspect of the far-forward detector acceptance is the ability of the far-forward detectors to enable “double-tagging”, where both the spectator neutron and leading (active) proton are tagged and reconstructed in the final state. The momentum transfer, t , distribution is shown in the right-most panel of Fig. 6. Fourier-transforming this t -distribution enables a spatial imaging program to be carried out for the gluons in the deuteron, where the spectator kinematics can be used to control the nuclear effects present in the nucleus and further permit the study of gluon structure as a function of nuclear configuration.

3.3. Free neutron structure

Access to the structure of a free neutron is experimentally challenging due to the impossibility of circulating bare neutrons in a collider. The only option is to use light nuclei (*e.g.* deuterons or ^3He) as proxies for a neutron beam, generating a susceptibility to nuclear binding effects and Fermi motion in the nucleus. The procedure of pole extrapolation on the deuteron, illustrated in [14–16], is one way to extract free neutron structure from a deuteron. This procedure allows for extrapolation of the reduced cross section of the nucleon to the on-shell point of the deuteron wavefunction ($p_{T,p}^2 \rightarrow -a_T^2$), where $a_T^2 = m_N^2 - \alpha_p(\alpha_p - 2)\frac{m_D^2}{4}$ and α_p , m_D , and m_N are the light-cone momentum fraction, deuteron mass, and average nucleon mass, respectively. This approach takes advantage of the properties of the deuteron spectral function and the pole of the spectral function, which are equal at the on-shell point. The extrapolation procedure enables extraction of the free neutron (or proton) structure functions, free of nuclear binding effects, and final-state interactions. Figure 7 shows a cartoon depicting the nuclear configurations and kinematic relations, and the effect of the extrapolation to the on-shell point.

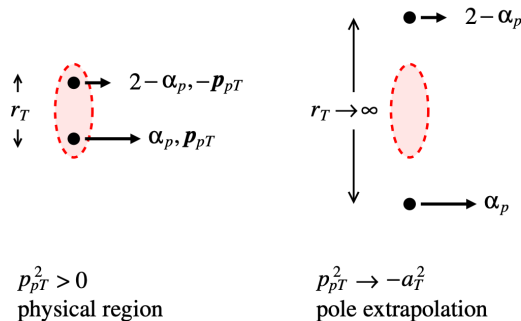


Fig. 7. Cartoon depicting bound deuteron nucleus (left) and free nucleons (right) after pole extrapolation to the on-shell point of the deuteron wave function. From [16].

A study of the experimental prospects of this procedure at the EIC was presented in [17]. The main conclusion of the study shows that the measurement can be carried out for extraction of both free neutron and free proton structure functions, with the latter enabling comparison to free proton measurements in $e + p$ to carefully evaluate systematic uncertainties associated with the extrapolation procedure and the detector effects. Figure 8 shows the results for both the free neutron and proton structure at the generator level and with a full reconstruction of kinematics via **Geant4** simulations of the EIC far-forward region described in Section 2. The extrapolation is done with a 1st-degree polynomial fit, and relies on tagging of the spectator protons/neutrons at $p_T \sim 0$ MeV/ c to reduce uncertainty in the fitting and extrapolation procedure, something unique to the EIC collider kinematics *versus* fixed-target experiments.

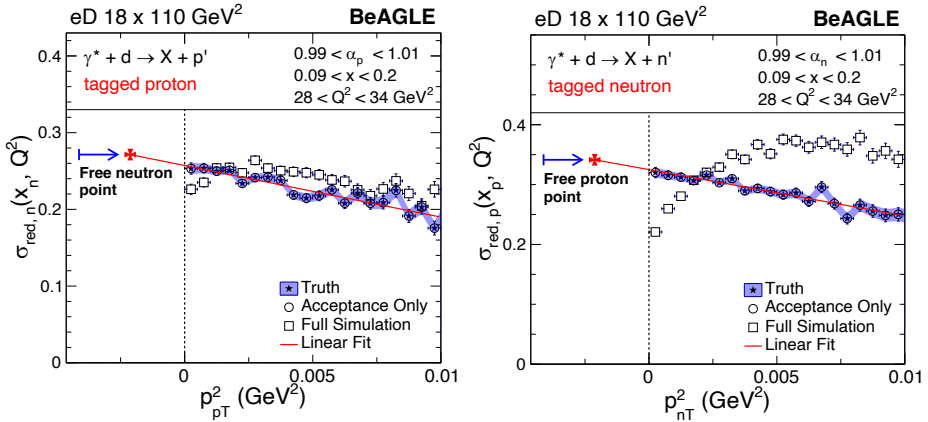


Fig. 8. Reduced cross section for active nucleons using tagged spectators to extract free nucleon structure functions. The tagged proton spectator (left) yields access to the neutron structure functions, while tagged spectator neutrons provide the free proton structure. Detector effects can be seen as distortions of the MC distributions from BeAGLE, and are worse for the tagged neutron given the worse momentum resolution from the ZDC compared to the silicon tracking detectors used for the spectator proton reconstruction. From [17].

3.4. Tagged-EMC effect

The EMC effect was discovered by the European Muon Collaboration in the 1980s [18] and it deepened the mystery in our understanding of modifications to nuclear structure at high Bjorken- x ($0.3 < x < 0.7$). In the past 40 years, many experiments have been carried out with an aim of finally understanding the origin of the EMC effect, but no definitive answer has been established to date. As seen in the studies summarized in Sections 3.2

and 3.3, the kinematic access to tagged DIS at the EIC also affords the capability to study the EMC effect, with the enhanced coverage in phase space required to differentially study various nuclear configurations and study the onset of nuclear modifications.

Continuing the theme of using the deuteron as our hadron beam, the idea has been proposed to focus on the virtuality dependence of the nucleons in the deuteron to control the EMC effect, with the assumption that the off-shellness of the nucleons contributes to the observed EMC effect [19, 20]. A cartoon of the different nuclear configurations is shown in Fig. 9.

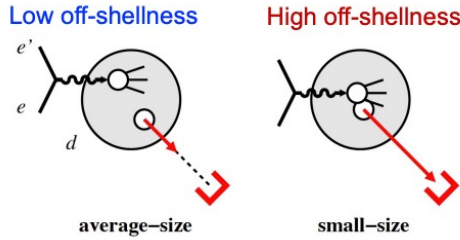


Fig. 9. Cartoon illustration of an average- and small-size deuteron, where nuclear effects are maximized in the latter case, where the nucleons are at very high virtuality.

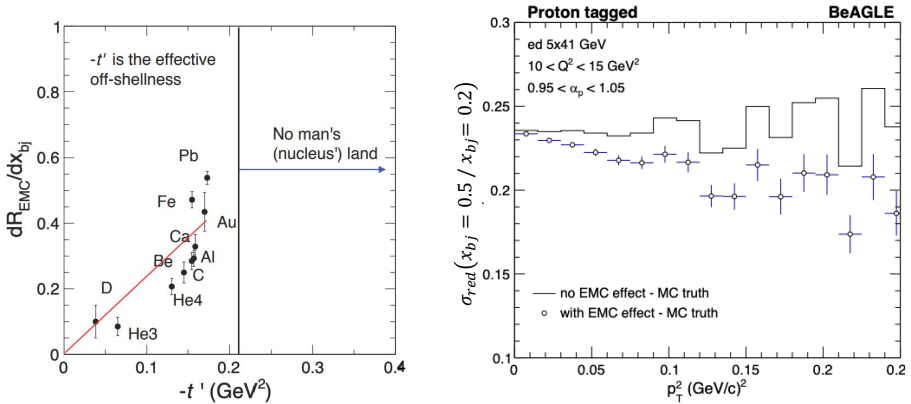


Fig. 10. The left panel shows EMC slope values extracted from the experiment for various nuclei, plotted as a function of the average nucleon virtuality. The dependence is then fit with a 1st-degree polynomial to parametrize the virtuality dependence of the EMC effect for inclusion in the BeAGLE events. The right panel shows the cross-section ratio between $x_n = 0.5$ and $x_n = 0.2$, which shows the shape difference of the ratio with and without the EMC weight included. No final-state interactions are included here.

To study the influence of the EMC effect in terms of the off-shellness, a minimal parametrization [19] of data for the EMC slope for various nuclei [21] was calculated (see Fig. 10), and this parametrization was then applied to the BeAGLE events as an event weight.

Once this parametrization was applied, an observable was constructed by taking the ratio of the deuteron reduced cross section in an x -region outside of the EMC region ($x = 0.2$) that also avoids the anti-shadowing region to that in a region of x which is clearly within the EMC region ($x = 0.5$). This ratio is shown in Fig. 10. The separation between the case with the EMC weight and that without gives a qualitative understanding of the statistical power required to observe the virtuality-dependent modification of the cross-section ratio. It should be noted that final-state interactions are expected to be large here as well and they are not yet included in this calculation.

4. Conclusions

The ePIC detector is designed to deliver a robust and exciting physics program for the EIC and drastically advance our understanding of the structure of matter. The far-forward instrumentation planned for installation as part of ePIC enables access to numerous exclusive final states and their associated observables, and is comprised of many cutting-edge detector technologies. The far-forward detectors are crucial to realise the full scientific potential of the EIC, and the science case for this suite of detectors has been broadened in recent years to include topics relevant to advance our knowledge of nuclear structure, in addition to the 3D partonic imaging program envisioned in the original EIC supporting documents. The community looks forward to the completion of the EIC construction so we can begin to answer some of nature's deepest mysteries.

The author would like to acknowledge his colleagues in the ePIC Collaboration, especially those from the far-forward detector working group.

REFERENCES

- [1] R. Abdul Khalek *et al.*, *Nucl. Phys. A* **1026**, 122447 (2022), [arXiv:2103.05419](https://arxiv.org/abs/2103.05419) [physics.ins-det].
- [2] J. Adam *et al.*, «Electron Ion Collider Conceptual Design Report», https://www.bnl.gov/ec/files/EIC_CDR_Final.pdf
- [3] A. Accardi *et al.*, [arXiv:1212.1701](https://arxiv.org/abs/1212.1701) [nucl-ex].
- [4] ePIC Collaboration, DD4hep based Geant 4 simulation package for the ePIC Collaboration Detector Simulations, <https://github.com/eic>

- [5] J. Adam *et al.*, *J. Instrum.* **17**, P10019 (2022).
- [6] J.K. Adkins *et al.*, [arXiv:2209.02580](#) [[physics.ins-det](#)].
- [7] W. Chang *et al.*, *Phys. Rev. D* **104**, 114030 (2021), [arXiv:2108.01694](#) [[nucl-ex](#)].
- [8] A. Kiselev, A. Jentsch, EICRoot: A light-weight Geant detector simulation software suite based on the FairRoot framework, <https://github.com/eic/EicRoot>
- [9] ALICE Collaboration, «Letter of Intent: A Forward Calorimeter (FoCal) in the ALICE experiment», CERN-LHCC-2020-009, LHCC-I-036, <https://cds.cern.ch/record/2719928/files/LHCC-I-036.pdf>
- [10] W. Chang *et al.*, *Phys. Rev. D* **106**, 012007 (2022).
- [11] T. Sjöstrand, S. Mrenna, P. Skands, *J. High Energy Phys.* **2006**, 026 (2006).
- [12] C. Ciofi degli Atti, S. Simula, *Phys. Rev. C* **53**, 1689 (1996).
- [13] Z. Tu *et al.*, *Phys. Lett. B* **811**, 135877 (2020).
- [14] M. Strikman, C. Weiss, *Phys. Rev. C* **97**, 035209 (2018).
- [15] M. Sargsian, M. Strikman, *Phys. Lett. B* **639**, 223 (2006).
- [16] W. Cosyn, C. Weiss, *Phys. Rev. C* **102**, 065204 (2020).
- [17] A. Jentsch, Z. Tu, C. Weiss, *Phys. Rev. C* **104**, 065205 (2021).
- [18] European Muon Collaboration (J. Aubert *et al.*), *Phys. Lett. B* **123**, 275 (1983).
- [19] L. Frankfurt, M. Strikman, *Nucl. Phys. B* **250**, 143 (1985).
- [20] C. Ciofi degli Atti, L.L. Frankfurt, L.P. Kaptari, M.I. Strikman, *Phys. Rev. C* **76**, 055206 (2007).
- [21] J. Seely *et al.*, *Phys. Rev. Lett.* **103**, 202301 (2009).